4C.4 Eywall Replacement Cycle of Hurricane Matthew (2016) observed by Doppler radar

Ting-Yu Cha* and Michael M. Bell

Department of Atmospheric Science, Colorado State University, Fort Collins, CO

1. INTRODUCTION

Eyewall replacement cycle (ERC) is a key process in tropical cyclone (TC) intensity and structure changes. The weakening inner eyewall is replaced by strengthening, contracting outer eyewall during an ERC. Several studies outlined a paradigm of classic ERC in an axisymmetric framework which is often associated with three phases: intensification, weakening and reintensification (Sitkowski et al. 2011). The broadening of the maximum tangential wind can cause profound impacts both on storm surge and wind fetch. This replacement mechanism plays an important role in the oscillations of intensity and is still not fully understood due to a lack of detailed observations.

Previous studies have shown that the eyewall replacement in axisymmetric framework captures the governing processes. However, not too many studies discussed the contribution of asymmetric processes in ERC. Reasor et al. 2000 suggested that sheared vortex Rossby waves caused a structural evolution in the inner core of hurricane Olivia (1994). Hurricane Gonzalo (2014) exhibited the azimuthal shift of maximum low-level inflow and updrafts in ERC evolution in a shear-relative quadrant (Didlake et al. 2017).

Hurricane Matthew (2016) was observed by the NEXRAD KAMX, KMLB, and KJAX WSR-88D S-band polarimetric radars for 35 hours with high temporal resolution and NOAA P-3 airborne radar with high spatial resolution when it approached southeastern United States during an ERC event, providing a new dataset with which to better understand the ERC process. The radar observations indicate that Matthew's primary eyewall was replaced with a weaker outer eyewall, but unlike a classic ERC, Matthew did not reintensify after the inner eyewall disappeared and the storm was dominated by wavenumber 1 asymmetries. The Generalized Velocity Track Display (GVTD) (Jou et al. 2008) was utilized to diagnose the vortex axisymmetric and asymmetric structure from single Doppler ground-based radar.

In this study, we examined the role of vertical wind shear and low-wavenumber evolution in Matthew's ERC event with triple Doppler and single Doppler analyses.

2. DATA AND METHODOLOGY

Hurricane Matthew was under the NEXRAD KAMX, KMLB, and KJAX ground-based radars surveillance range for 35 hours from 19 UTC 6 October to 00 UTC 8 October (Fig. 1). We conducted GVTD technique with high temporal resolution to retrieve the axisymmetric and wavenumber 1 tangential wind every 6 minutes. The hurricane center finding algorithm is based on the GVTD-simplex (Lee and Marks Jr 2000).

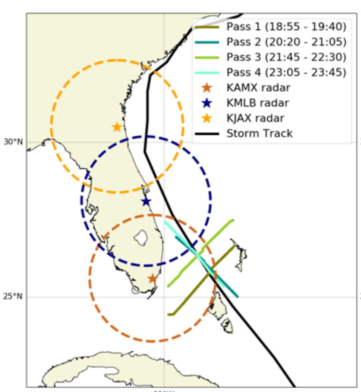

FIG. 1. Pass 1-4 denote the passage of P-3 plane across the cyclone on Oct. 6th. Colored circles and stars represent the detecting range of single Doppler radar. Black line is the storm track.

Corresponding author address: Ting-Yu Cha, Colorado State University, Dept. of Atmospheric Science, 3915 W. Laporte Ave., Fort Collins, CO 80521;
e-mail: tingyu@colostate.edu

However, asymmetric component of radial wind is ignored in this method since the numbers of unknown variables are greater than the number of equations. Techniques to resolve the asymmetric radial wind are currently under investigation.

In addition to the ground-based radars, a NOAA P-3 aircraft mission was conducted during 19 UTC 6 Oct. to 0 UTC 7 Oct. Combining the tail radar with fore/aft scanning technique and KAMX radar, triple Doppler analysis was performed by SAMURAI (Bell et al. 2013). The low-wavenumber structure was deduced from reflectivity and wind composites by performing linear least squares fit (Lee et al. 2000) with the restriction of maximum allowable gap size (Lorsolo and Aksoy 2012). We also utilized the 850-200-hPa deep-layer environmental vertical wind shear, which is from the Statistical Hurricane Intensity Prediction Scheme (SHIPS) database.

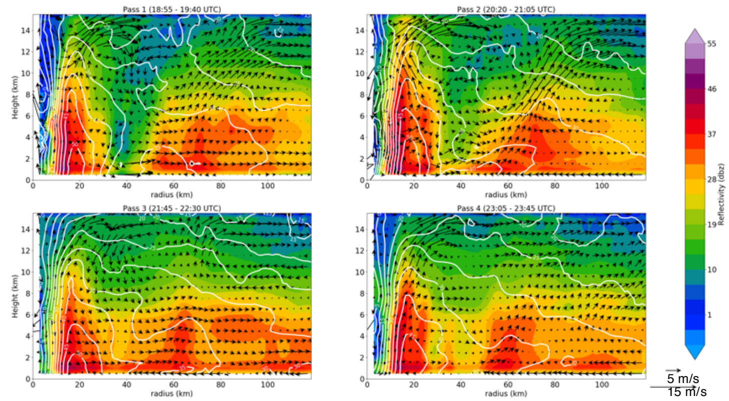

FIG. 3. Axisymmetric reflectivity (shaded), primary circulation (white contour, m/s) and secondary circulation (vector) derived from P-3 tail radars and KAMX radar.

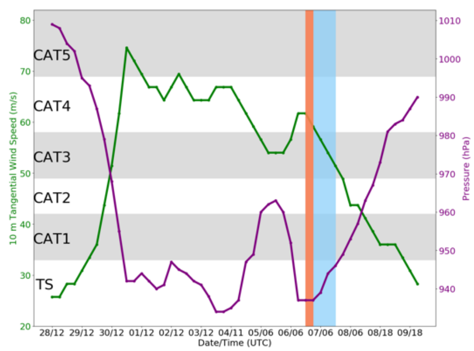

FIG. 2. Central pressure and maximum wind speed throughout the lifetime of Matthew. Orange line represents the analysis period of triple Doppler analysis (6th/19Z-7th/00Z). Light blue shaded represents the analysis period of single Doppler analysis (6th/19Z-8th/00Z).

3. RESULTS AND DISCUSSION

Figure 2 shows the National Hurricane Center best-track and intensity of Hurricane Matthew. Matthew went through rapid intensification and reached category 5 on 1 October. A secondary eyewall was first observed in the satellite imagery on 1656 UTC 6 October, and started to intensify. The operational reconnaissance flights observation captured the intensification and weakening stages of ERC and the single Doppler radar observations documented the ERC evolution.

3.1 Intensification stage of ERC

Four passes of the P-3 aircraft showed the evolution of the reflectivity, tangential winds and secondary circulation as the outer eyewall became well-established. Secondary eyewall vorticity was maximized at low-levels and closely coupled with low-level inflow, developing updraft, and convergence of angular momentum (FIG. 3). This is consistent with the axisymmetric intensification mechanism outlined by Smith et al. 2009, where radial convergence of angular momentum above the boundary layer spins up the outer circulation as the result of the balanced secondary circulation. This analysis result is also consistent with the kinematic evolution of the formation of secondary eyewall in Hurricane Rita (2005) (Bell et al. 2012).

3.2 Weakening and Reintensification stages of ERC

The single Doppler analyses indicate that the inner eyewall intensified between 2030 UTC to 2130 UTC 6 October, which was consistent with the pass 1 through pass 4 of the triple Doppler analysis. The inner eyewall decayed a few hours

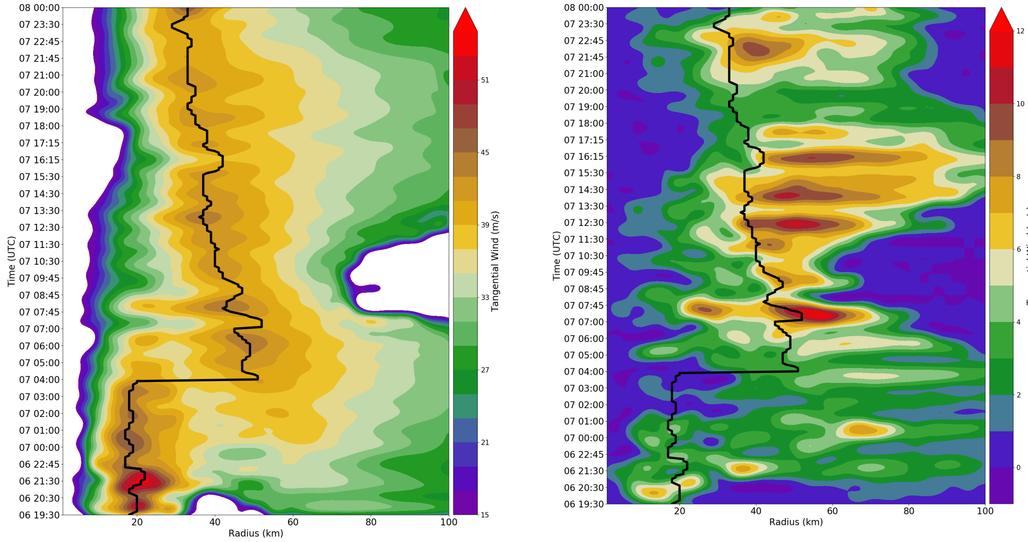

FIG. 4. Time/radius diagram of GVTD analysis of (a) axisymmetric tangential wind and (b) wavenumber-1 tangential wind from KAMX, KMLB and KJAX radars at altitude of 3 km. Black line denotes axisymmetric radius of maximum wind.

after the P-3 flight, while the outer eyewall contracted (FIG. 4a). The maximum tangential wind at 3 km of the outer eyewall started to surpass the maximum tangential wind of the inner eyewall from 4 UTC 7 October, suggesting that Matthew may have started the reintensification phase. However, Matthew did not reintensify and became more asymmetric over time. The wavenumber 1 component became significant and influenced the storm's structure (FIG. 4b).

3.3 Deep layer vertical wind shear played an important role in Hurricane Matthew's ERC

To further diagnose the reason of lack of reintensification of the outer eyewall, we examine the 850-200 hPa deep layer vertical wind shear. It shows that the intensification of the shear magnitude correlates well with the decaying intensity of the tangential wind speed. The above results suggest that increasing vertical wind shear played an important role in the ERC process and weakening of Matthew, leading to a different evolution from a classic ERC. More results will be presented in the conference.

4. REFERENCES

Bell, M. M., M. T. Montgomery, and W.-C. Lee, 2012: An Axisymmetric View of Concentric Eyewall Evolution in Hurricane Rita (2005). *J. Atmos. Sci.*, **69**, 2414–2432, doi:10.1175/JAS-D-11-0167.1. http://journals.ametsoc.org/doi/abs/10.1175/JAS-D-11-0167.1.

——, W. C. Lee, C. A. Wolff, and H. Cai, 2013: A solo-based automated quality control algorithm for airborne tail Doppler radar data. *J. Appl. Meteorol. Climatol.*, **52**, 2509–2528, doi:10.1175/JAMC-D-12-0283.1.

Didlake, A. C., G. M. Heymsfield, P. D. Reasor, and S. R. Guimond, 2017: Concentric Eyewall Asymmetries in Hurricane Gonzalo (2014) Observed by Airborne Radar. *Mon. Weather Rev.*, **145**, 729–749, doi:10.1175/MWR-D-16-0175.1. http://journals.ametsoc.org/doi/10.1175/MWR-D-16-0175.1.

Jou, B. J.-D., W.-C. Lee, S.-P. Liu, and Y.-C. Kao, 2008: Generalized VTD Retrieval of Atmospheric Vortex Kinematic Structure. Part I: Formulation and Error Analysis. *Mon. Weather Rev.*, **136**, 995–1012, doi:10.1175/2007MWR2116.1. http://journals.ametsoc.org/doi/abs/10.1175/2007MWR2116.1.

Lee, W.-C., and F. D. Marks Jr, 2000: Tropical cyclone kinematic structure retrieved from single-Doppler radar observations. Part II: The GBVTD-simplex center finding algorithm. *Mon. Weather Rev.*, **128**, 1925–1936, doi:10.1175/1520-0493(2000)128<1925:TCKSRF>2.0.CO;2. http://journals.ametsoc.org/doi/abs/10.1175/1520-0493(2000)128%3C1925:TCKSRF%3E2.0.CO;2%5Cnhttp://journals.ametsoc.org/doi/pdf/10.1175/1520-0493(2000)128%3C1925:TCKSRF%3E2.0.CO;2.

——, B. J.-D. Jou, P.-L. Chang, and F. D. Marks, 2000: Tropical Cyclone Kinematic Structure Retrieved from Single-Doppler Radar Observations. Part III: Evolution and Structures of Typhoon Alex (1987). *Mon. Weather Rev.*, **128**, 3982–4001, doi:10.1175/1520-0493(2000)129<3982:TCKSRF>2.0.CO;2. http://dx.doi.org/10.1175/1520-0493(2000)129%3C3982:TCKSRF%3E2.0.CO%5Cnhttp://0.0.0.2.

Lorsolo, S., and A. Aksoy, 2012: Wavenumber Analysis of Azimuthally Distributed Data: Assessing Maximum Allowable Gap Size. *Mon. Weather Rev.*, **140**, 1945–1956, doi:10.1175/MWR-D-11-00219.1. http://journals.ametsoc.org/doi/abs/10.1175/MWR-D-11-00219.1.

Reasor, P. D., M. T. Montgomery, F. D. Marks, and J. F. Gamache, 2000: Low-Wavenumber Structure and Evolution of the Hurricane Inner Core Observed by Airborne Dual-Doppler Radar. *Mon. Weather Rev.*, **128**, 1653–1680, doi:10.1175/1520-0493(2000)128<1653:LWSAEO>2.0.CO;2.

Sitkowski, M., J. P. Kossin, and C. M. Rozoff, 2011: Intensity and Structure Changes during Hurricane Eyewall Replacement Cycles. *Mon. Weather Rev.*, **139**, 3829–3847, doi:10.1175/MWR-D-11-00034.1. http://journals.ametsoc.org/doi/abs/10.1175/MWR-D-11-00034.1.

Smith, R. K., M. T. Montgomery, and N. Van Sang, 2009: Tropical cyclone spin-up revisited. **1335**, 1321–1335, doi:10.1002/qj.